

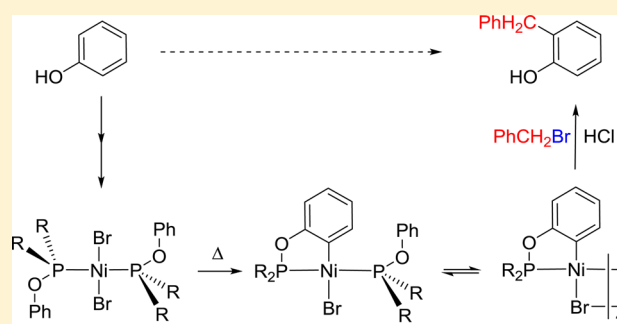
Ortho Derivatization of Phenols through C–H Nickelation: Synthesis, Characterization, and Reactivities of Ortho-Nickelated Phosphinite Complexes

Boris Vabre, Félix Deschamps, and Davit Zargarian*

Département de chimie, Université de Montréal, Montréal, Québec, Canada H3C 3J7

S Supporting Information

ABSTRACT: Reported here are the synthesis and characterization of ortho-nickelated complexes derived from phosphinite ligands and investigated as model compounds in the development of C–H functionalization strategies for arenol substrates. Reaction of *i*-Pr₂POPh with 0.6 equiv of [(*i*-PrCN)NiBr₂]_{*n*} and 0.8 equiv of NEt₃ in toluene (100 °C, 36 h) gave the yellow, monomeric cyclometalated complex *trans*-{κ²P,C-C₆H₄OP(*i*-Pr)₂}Ni(*i*-Pr₂POPh)Br (**3a**) in 93% yield. The closely related yellow-orange dimeric species [{κ²P,C-C₆H₄OP(*i*-Pr)₂}Ni(μ-Br)]₂ (**4a**) was obtained in 70% yield when *i*-Pr₂POPh was treated with 2 equiv each of the Ni precursor and NEt₃. These complexes have been characterized fully and shown to interconvert in the presence of excess ligand (**4a** → **3a**) or excess Ni precursor (**3a** → **4a**). Treatment of **3a** or **4a** with benzyl bromide at 90 °C over extended periods led to benzylation of the Ni–aryl moiety in these complexes. Examination of the cyclometalation pathway for *i*-Pr₂POPh has shown that the first species formed from its ambient-temperature reaction with [(*i*-PrCN)NiBr₂]_{*n*} is *trans*-(*i*-Pr₂POPh)₂NiBr₂ (**2a**). NMR studies showed that **2a** undergoes a rapid ligand exchange at room temperature, which can be slowed down at –68 °C; this fluxional process shifts in the presence of NEt₃, implying the partial formation of an amine adduct. Heating toluene mixtures of **2a** and NEt₃ at 90 °C for 38 h led to the formation of **3a** via C–H nickelation. That phosphinite dissociation from **2a** precedes the C–H nickelation step is implied by the observation that the formation of **3a** is hindered in the presence of excess *i*-Pr₂POPh. The impact of phenol ring substituents on the C–H nickelation rate was probed by preparing substituted derivatives of **2a**, *trans*-(4-R-C₆H₄OP(*i*-Pr₂))₂NiBr₂ (R = OMe (**2b**), Me (**2c**), COOMe (**2d**)), and measuring their relative rates of C–H nickelation. These studies showed that the formation of cyclonickelated products is favored in the order COOMe < Me < OMe, which is consistent with an electrophilic nickelation mechanism. Studying the C–H nickelation of 3-F-C₆H₄OP(*i*-Pr₂) allowed us to establish that metalation is favored at the para position with respect to F (85:15).

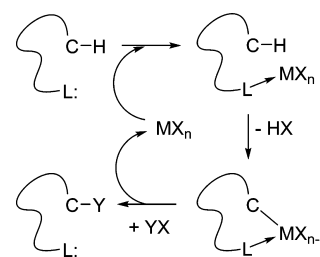


INTRODUCTION

Synthetic strategies based on C–H functionalization have grown in prominence and constitute a central part of the current global drive to develop sustainable chemical processes.¹ The most facile and common strategy in the area of metal-catalyzed C–H metalation relies on the presence in substrates of nucleophilic moieties that can bind the metal atom to facilitate its interaction with the C–H moiety to be activated. This type of chelation-assisted approach based on “functional directing groups” is commonly assumed to generate metallacycles as key intermediates that react subsequently with cosubstrates to give the products of functionalization (Scheme 1).

Whereas most C–H functionalization methodologies are based on one-pot approaches that bypass isolation or even detection of reaction intermediates, there are potentially significant benefits in intercepting the initial cyclometalated species and investigating the main factors influencing their formation, stability, and reactivities. Any knowledge gained

Scheme 1. Idealized Scheme for Chelation-Assisted, Direct Functionalization of C–H Bonds



from such studies should improve our understanding of the important steps involved in catalytic C–H functionalization processes and help develop more efficient methodologies.

Received: September 11, 2014

Published: November 4, 2014

A survey of the C–H functionalization literature reveals that most of the early successes in this area hinged on the use of the noble metals Ru,² Rh and Ir,³ and Pd,⁴ but a recent drive toward more sustainable C–H functionalization strategies has led to greater use of the more abundant 3d counterparts of the above-noted noble metals, namely Fe,⁵ Co,⁶ and Ni.⁷ The use of Ni precursors in this context also has a historic significance, since Ni was one of the earliest metals to show an aptitude in C–H metalation.⁸ These considerations and our group's longstanding interest in organonickel chemistry⁹ have inspired us to initiate projects aimed at developing C–H functionalization methodologies based on Ni precursors.

In light of the aforementioned importance of metallacycles, we have set out to prepare nickelacyclic complexes via C–H nickelation and study their ease of formation, structures, and reactivities as part of a long-term strategy aimed at developing Ni-based C–H functionalization methodologies. An initial search of the literature revealed that very few metallacyclic complexes of Ni have been reported previously, especially in comparison to the much better known analogues based on Pd and Pt. Representative examples of reported nickelacycles include complexes based on aromatic Schiff bases and benzyl amines,¹⁰ as well as aromatic phosphines¹¹ and phosphinites.^{12,13} It is noteworthy that these nickelacyclic complexes have all been prepared by oxidative addition of C–X bonds (X = Br, Cl) to Ni(0) precursors and not via direct C–H nickelation. To our knowledge, no nickelacyclic complex (excluding pincer systems) has been prepared via C–H nickelation; this presents an opportunity for developing C–H nickelation based routes to nickelacyclic systems.

We have elected to begin our studies by examining the C–H functionalization of phosphinite ligands derived from phenol and its substituted derivatives, because this approach would let us capitalize on our experience in the synthesis and reactivities of pincer complexes of nickel based on bis(phosphinites).¹⁴ An important advantage of a phosphinite directing group in C–H functionalization is its facile preparation from alcohols and ClPR₂, which would give access to a potentially large and diverse family of substrates. In addition, a phosphinite moiety can be removed readily by a number of simple workup strategies, thus qualifying this strategy as a so-called “traceless” functionalization.¹⁵ There are literature precedents for the use of phosphinites in C–H functionalization using Ru,¹⁶ Rh,¹⁷ and Pd,¹⁸ but none with Ni.

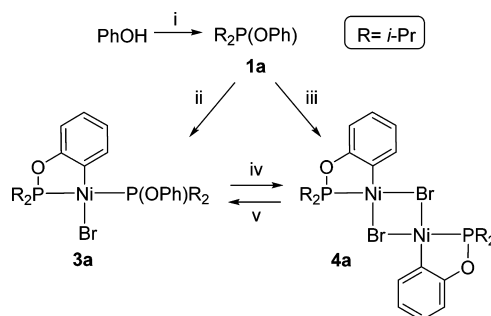
The present report describes the synthesis and full characterization of the ligands R–C₆H₄OP(*i*-Pr)₂ (R = H (**1a**), 4-OMe (**1b**), 4-Me (**1c**), 4-CO₂Me (**1d**), 3-F (**1e**)) and their bis-adducts *trans*-{R–C₆H₄OP(*i*-Pr)₂}₂NiBr₂ (R = H (**2a**), OMe (**2b**), Me (**2c**), CO₂Me (**2d**)). Cyclonickelation of **1a** gave the complexes *trans*-{κ²P,C–C₆H₄OP(*i*-Pr)₂}Ni(*i*-Pr₂POPh)Br (**3a**) and [{κ²P,C–C₆H₄OP(*i*-Pr)₂}NiBr(μ-Br)]₂ (**4a**), which were fully characterized and used in functionalization tests with benzyl bromide to give 2-benzylphenol and its phosphinated derivatives. Also described herein are the influence of aryl substituents (OMe, Me, COOMe) on C–H nickelation rates and site selectivity in the nickelation of 3-fluorophenol.

RESULTS AND DISCUSSION

Synthesis and Characterization of Ortho-Nickelated Complexes Derived from Phenol. Treating phenol with *i*-Pr₂PCl and NEt₃ in THF gave the phosphinite ligand **1a** (room temperature, 1 h, 90%),¹⁸ which was then used for the synthesis

of the target cyclometalated complexes, as follows. Refluxing a toluene mixture of **1a**, 0.6 equiv of our Ni precursor [(*i*-PrCN)NiBr₂]_n¹⁹ and 0.8 equiv of NEt₃ gave a yellow solid identified as **3a** in 93% yield, whereas using 2 equiv each of the Ni precursor and base gave the closely related yellow-orange dimeric species **4a** in 70% yield (Scheme 2). Complex **4a** reacts

Scheme 2. Synthesis of Cyclometalated Complexes of Ni^a



^aConditions: (i) R₂PCl, NEt₃, THF, room temperature, 1 h; (ii) 0.6 [(*i*-PrCN)NiBr₂]_n, 0.8 NEt₃, toluene, 100 °C, 36 h; (iii) 2.0 [(*i*-PrCN)NiBr₂]_n, 2.0 NEt₃, toluene, 100 °C, 40 h; (iv) excess [(*i*-PrCN)NiBr₂]_n, excess NEt₃, toluene, 100 °C, 40 h; (v) **1a** (1.0 equiv), C₆D₆, room temperature, 5 min.

readily at room temperature with 1 equiv of **1a** to give its phosphinite adduct **3a**, whereas heating the latter in the presence of excess Ni precursor and base cleanly furnishes **4a**. This interconversion is significant for understanding the cyclometalation pathway (vide infra).

The new complexes **3a** and **4a** have been characterized fully. The ³¹P{¹H} NMR spectrum of **4a** shows a sharp singlet at 199 ppm, downfield of the corresponding signal for the free ligand (149 ppm). Complex **3a** showed the anticipated AB doublets at ca. 185 and 152 ppm for the cyclometalated and non-cyclometalated phosphinite moieties, respectively; the large ²J_{PP} value of 325 Hz for these resonances is typical of nonequivalent phosphinites in mutually *trans* positions.^{17,19} The ¹³C resonance for C_{ipso} in **3a** appeared as a doublet of doublets at 132 ppm (²J_{CP} = 14 and 29 Hz), whereas a complex multiplet was observed for the corresponding signal in **4a**.

X-ray diffraction studies carried out on single crystals of **3a** and **4a** confirmed the solid-state structures of these complexes (Figure 1). The Ni center in both complexes adopts a square-planar geometry distorted by the five-membered metallacycle. The different steric demands of the two phosphinite ligands in **3a** also lead to structural distortions. For instance, the P atom belonging to the noncyclometalated phosphinite moiety forms larger *cis* angles relative to the corresponding angles involving the P atom of the cyclometalated phosphinite moiety: 101 vs 83° for C–Ni–P and 92 vs 86° for P–Ni–Br. The same phenomenon is observed in **4a**: C1–Ni–P1 is much narrower than C1–Ni–Br1 (ca. 98°). The *trans* angles in **4a** and the P1–Ni–P2 angle in **3a** are not affected much (174–176°); the latter is much larger than the corresponding angle in POCOP complexes.²⁰ On the other hand, the C–Ni–Br angle of 165° in **3a** is much smaller than the ideal value expected for a *trans* angle, presumably due to steric repulsions between Br and the noncyclometalated phosphinite.

Inspection of the bond distances in **3a** and **4a** reveals interesting observations on the impact of cyclometalation. In **3**, for example, the chelate effect of the cyclometalated moiety

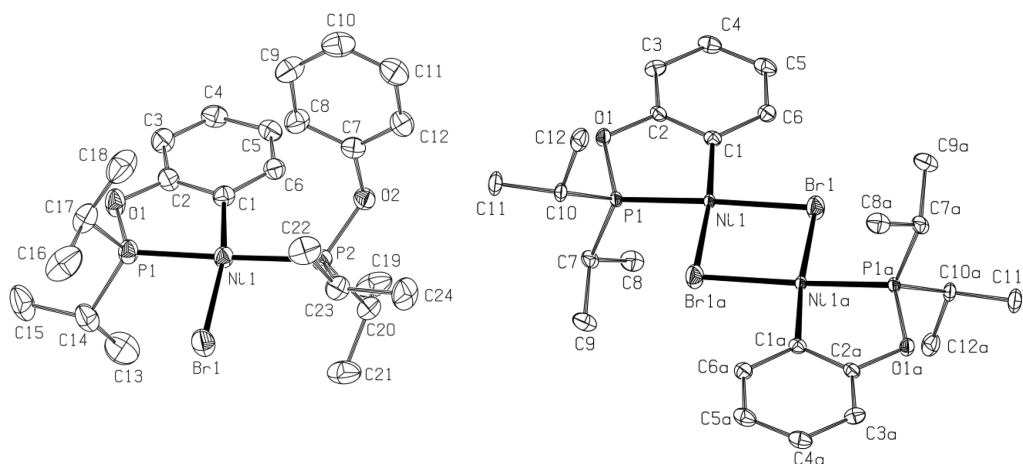
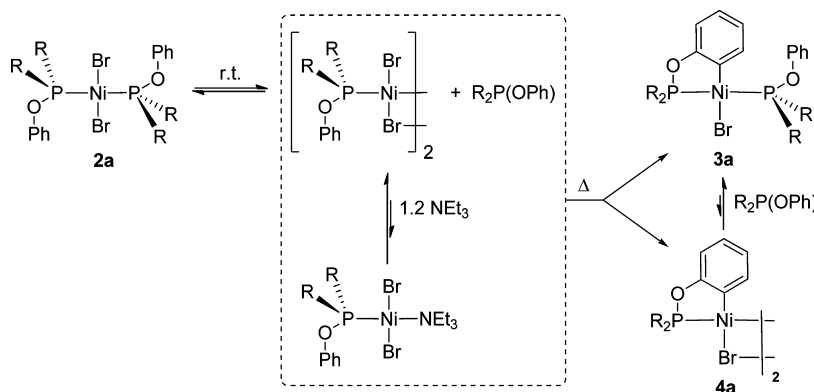


Figure 1. Structure diagrams for complexes **3a** (left) and **4a** (right). Thermal ellipsoids are shown at the 50% probability level. Hydrogen atoms are omitted for clarity. Selected bond distances (Å) and angles (deg): Ni–C1 = 1.935(2) (**3a**), 1.914(4) (**4a**); Ni–P1 = 2.1359(5) (**3a**), 2.0953(10) (**4a**); Ni–P2 = 2.2510(5) (**3a**); Ni–Br1 = 2.3664(3) (**3a**), 2.3641(7) (**4a**); Ni–Br1a = 2.3771(7) (**4a**); C1–Ni–Br1 = 164.92(5) (**3a**), 97.61(12) (**4a**); C1–Ni–Br1a = 174.24(12) (**4a**); P–Ni–P = 172.97(2) (**3a**); C1–Ni–P1 = 82.96(5) (**3a**), 82.07(12) (**4a**); C1–Ni–P2 = 100.83(5) (**3a**); Br1a–Ni–P1 = 92.62(3) (**4a**); Br1–Ni–P1 = 85.564(15) (**3a**), 176.19(4) (**4a**); Br1–Ni–P2 = 91.632(15) (**3a**); Br1–Ni–Br1a = 87.84(2) (**4a**).

Scheme 3. Proposed Ligand Dissociation and Exchange/Cyclometalation Process in the Presence of NEt_3



results in a shorter Ni–P distance for P1 relative to P2 (2.14 vs 2.25 Å). An even shorter Ni–P distance is observed for the cyclometalated moiety in **4a** relative to **3a** (2.10 vs 2.14 Å), which can be attributed to two factors. First, P1 is trans from a weaker ligand in **4a** in comparison to that in **3a** (Br < ArOPR₂). A second factor might be the decreased overall electron donation to the Ni center when the nonmetalated phosphinite moiety in **3a** is replaced by a bridging Br in **4a**: the shorter Ni–P distance in the latter would thus compensate for this change. This phenomenon would also rationalize the significantly shorter Ni–C distance observed in **4a** in comparison to **3a** (1.91 vs 1.94 Å).

Elucidation of C–H Nickelation Pathway. The pathway(s) leading to complexes **3a** and **4a** were examined with the objective of detecting intermediates and identifying the factors influencing the C–H metalation step. Described below are our attempts to intercept and characterize the species forming initially on the path to cyclometalation.

Stirring a toluene mixture of the ligand **1a** and 0.5 equiv of $[(i\text{-PrCN})\text{NiBr}_2]_n$ at room temperature led immediately to formation of a dark brown solution displaying a broad ³¹P singlet at 136 ppm, which is presumably due to a fluxional process involving exchange of the phosphinite ligand. Single crystals grown at –37 °C (deep yellow, 82% yield) were subjected to X-ray diffraction studies that allowed us to identify

the product as the bis(phosphinite) complex *trans*-(*i*-Pr₂P(OPh)₂)₂NiBr₂ (**2a**). The structural parameters for this square-planar compound are unexceptional and will be discussed below along with the solid-state structures of its substituted derivatives (*vide infra*).

To shed some light on the aforementioned fluxional process, we examined the low-temperature NMR spectra of **2a** (CD₂Cl₂). The room-temperature ³¹P{¹H} NMR spectrum (Figure S1, Supporting Information) showed a broad singlet at 136 ppm (fwhm ≈ 760 Hz) that sharpened to a fine signal at –68 °C (Figure S1). Similar observations have been reported for the analogous complexes *trans*-(PR₃)₂NiBr₂ (PR₃ = *i*-Pr₂PMe, *i*-Pr₂PPh), which also undergo fast ligand exchange.²¹ The upfield region of the room-temperature ¹³C{¹H} NMR spectrum of **2a** (Figure S2, Supporting Information) also showed a somewhat broad singlet for PCH(CH₃)₂, whereas cooling to –68 °C led to appearance of the anticipated virtual triplet (29 ppm, *v*_{JPC} = 12 Hz).

With the objective of examining the above ligand exchange process under conditions relevant to the cyclometalation reaction, we prepared a toluene sample of **2a** (0.065 M) containing 1.2 equiv of NEt₃ and analyzed it by ³¹P{¹H} NMR spectroscopy, with and without heating. The predominant signal in the ambient-temperature spectrum was the original broad singlet (ca. 136 ppm), but the presence of NEt₃ gave rise

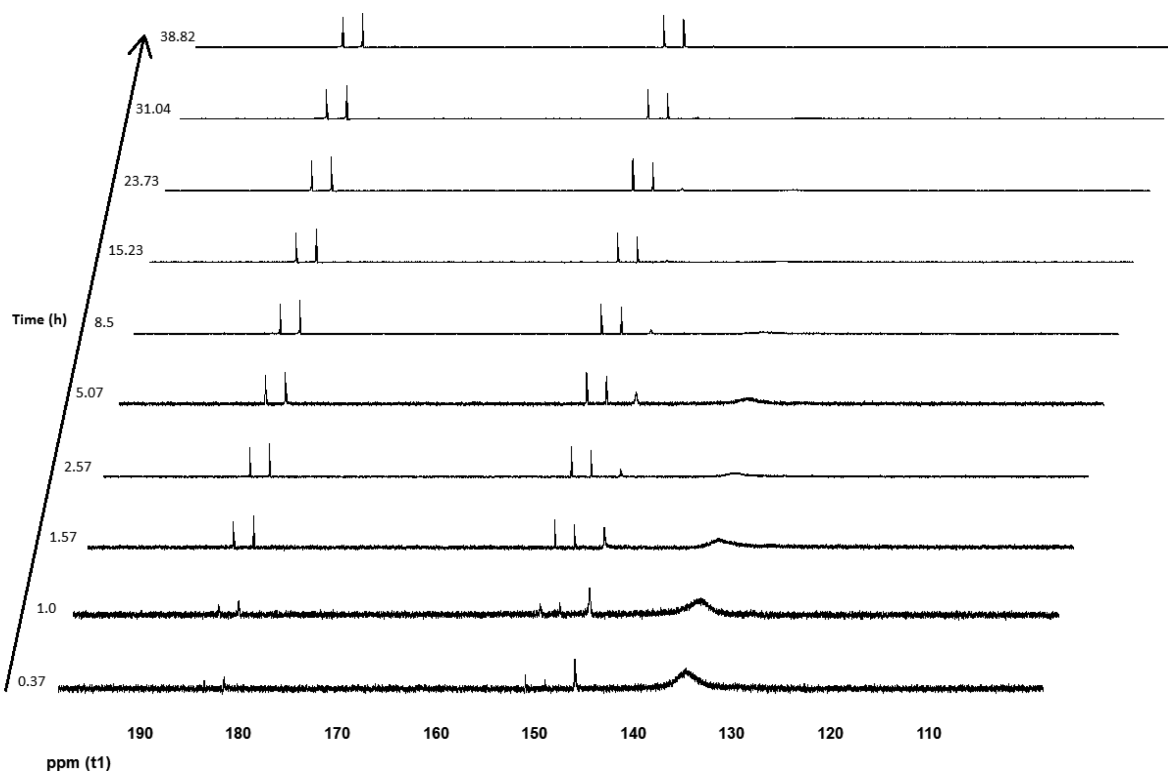


Figure 2. $^{31}\text{P}\{^1\text{H}\}$ NMR monitoring of a solution of **2a** (50 mg, 78 μmol) and NEt_3 (13 μL , 93.8 μmol) in toluene (1.2 mL) at 90 $^\circ\text{C}$ over 39 h.

to a second broad resonance at ca. 131 ppm as well as a sharp resonance at 147 ppm attributed to free ligand **1a** (Figure S3, Supporting Information); the integration ratio for these signals was approximately 20:1:1. We propose that the new broad singlet at ca. 131 ppm represents the phosphinite-depleted dimeric species $[(i\text{-Pr}_2\text{POPh})\text{BrNi}(\mu\text{-Br})_2]$ and its NEt_3 adduct $(i\text{-Pr}_2\text{POPh})(\text{NEt}_3)\text{NiBr}_2$, which are in equilibrium with each other and with **2a** (Scheme 3). Given the much weaker $\text{L}\rightarrow\text{Ni}$ binding force of NEt_3 relative to that of most P-based ligands, we believe it is unlikely that the substitution of the phosphinite ligand in **2a** is induced by NEt_3 ; instead, we propose that **2a** undergoes ligand dissociation to generate a dimeric intermediate that is then captured by NEt_3 , as shown in Scheme 3.

The spectrum of the toluene sample containing **2a** and NEt_3 discussed above remained virtually unchanged after 18 h at room temperature, indicating that the equilibrium governing the ligand exchange process is established at the time of mixing and that the cyclometalation requires higher temperatures. Heating this sample to 90 $^\circ\text{C}$ and monitoring by $^{31}\text{P}\{^1\text{H}\}$ NMR allowed us to observe the gradual process of cyclometalation (Figure 2). The original signals arising from the ligand exchange process discussed above, namely the broad signals at ca. 131 and 136 ppm and the sharp signal at 147 ppm, were slowly replaced by the AB doublets due to the cyclometalated species **3a**. At the same time, the dark brown reaction mixture faded gradually to a light yellow, and a white solid precipitated ($\text{HBr}\cdot\text{NEt}_3$).

^{31}P NMR spectroscopy was also used to monitor the gradual formation of cyclometalated products in the reaction of **1a** with $[(i\text{-PrCN})\text{NiBr}_2]_n$ and NEt_3 (molar ratio of 1:1:1; 90 $^\circ\text{C}$; Figure S4, Supporting Information). The predominant signal observed during the initial stages of this reaction was the broad singlet at ca. 136 ppm representing **2a**, which indicates that this bis(phosphinite) species is the main species present in the

reaction mixture even when equimolar quantities of **1a** and the Ni precursor are employed. As above, we observe the gradual conversion of **2a** to the cyclometalated products **3a** (AB doublets at ~ 185 and 152 ppm) and **4a** (a singlet at ~ 197 ppm) in the presence of NEt_3 . The preferential formation of **4a** over **3a** is expected because of the 1:1 ratio of **1a** to Ni employed, but the observed broadness of the signals due to **2a**–**4a** indicates that all of these species are in dynamic exchange as long as free **1a** is present in the reaction mixture. Indeed, the only sharp signal detected in the process is the singlet due to **4a** (198 ppm), which appears at the very end of the experiment as the sole P-bearing species. We conclude, therefore, that cyclometalation is the only irreversible step in this process (Scheme 3).

An important question that remains to answer is whether or not the cyclometalation step involves the phosphinite-depleted dimeric intermediate $[(i\text{-Pr}_2\text{POPh})\text{Ni}(\text{Br})(\mu\text{-Br})_2]$ postulated above; in other words, is the observed phosphinite dissociation equilibrium a required step for the cyclometalation? We carried out the following experiments to shed some light on this issue. Four NMR tubes were charged with **2a** (89 μmol), NEt_3 (107 μmol), and 0, 4, 8, and 16 equiv of **1a** in toluene (500 μL); a sealed capillary containing a toluene solution of PPh_3 was placed in the tubes to serve as the external standard. The samples were heated to 90 $^\circ\text{C}$ for 12.5 h and analyzed by $^{31}\text{P}\{^1\text{H}\}$ NMR spectroscopy, with the following results: the formation of **3a** diminished in the presence of added ligand **1a** by 54%, 31%, 19%, and 8%, respectively, which suggests that dissociation of a phosphinite from **2a** is required for the cyclometalation step.

We have not succeeded in isolating the dimeric intermediate $[(i\text{-Pr}_2\text{POPh})\text{Ni}(\text{Br})(\mu\text{-Br})_2]$ postulated in Scheme 3. Similarly, C–H palladation of closely related triaryl phosphite ligands are also thought to involve such dimeric species,²² but none have

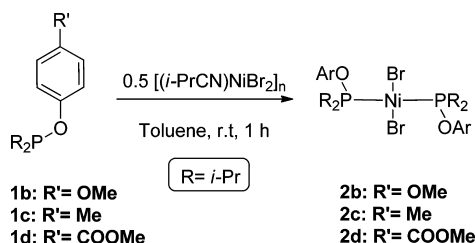
been isolated during these reactions. On the other hand, the complexes $[(R_3P)M(X)(\mu-X)]_2$ ($X = \text{halide}$) are known for Pd and Pt,²³ whereas a search of the literature has revealed no precedents for Ni, hinting that the latter might be inherently unstable.

Influence of Aryl Substituents on Cyclonickelation.

C–H metalation of aromatic substrates by MX_n can proceed through different mechanisms,²⁴ including the classical route involving successive steps of oxidative addition to give a hydrido aryl intermediate followed by reductive elimination of HX. While such a redox process seems a priori unlikely with a Ni(II) precursor, it is difficult to rule out this scenario experimentally. Another distinct possibility would be a so-called electrophilic (nonredox) process involving an initial binding of the C (or C–H) fragment followed by removal of H^+ by X^- . The latter process can take place in sequence or in a concerted manner, and it can be considered a σ -bond metathesis if there is little or no polarization of the C–H and M–X moieties at the transition state. Such an electrophilic mechanism is also difficult to establish unambiguously, but its likelihood can be evaluated when the impact of electronic factors on C–H nickelation rates is known. We have therefore examined the relative rates of C–H nickelation in substituted phenols in order to evaluate the electronic impact of substituents on cyclometalation rates, as described below.

The arenols 4-methoxyphenol, *p*-cresol, and methyl 4-hydroxybenzoate were used to prepare and isolate in 78–97% yields the corresponding phosphinites *i*-Pr₂PO(4-R-C₆H₄) (R = OMe (**1b**), Me (**1c**), CO₂Me (**1d**)), as described above for the parent ligand **1a** (THF/NEt₃, room temperature, 1 h). The ³¹P{¹H} NMR spectra of these ligands showed a singlet at ca. 150 ppm, characteristic of *i*-Pr₂POAr.^{18,19} In a manner analogous to the synthesis of **2a**, the new ligands were then treated with 0.5 equiv of $[(i\text{-PrCN})NiBr_2]_n$ at room temperature to give the bis(phosphinite) complexes *trans*-(*i*-Pr₂POAr)₂NiBr₂ (**2b–d**) (Scheme 4).

Scheme 4. Synthesis of **2b–d**



Toluene solutions of **2b–d** (0.16 mmol in 382 μ L; 0.042 M) containing 10 equiv of NEt₃ were then heated to 100 °C, and formation of the corresponding cyclometalated complexes **3b–d** was monitored by ³¹P NMR spectroscopy.²⁵ Integration of the resulting spectra allowed us to establish the aryl substituents' influence on nickelation (Figure S5, Supporting Information): after ca. 5 h, cyclometalation had progressed to a greater extent for complex **3b** (39%) relative to **3c** (32%) and **3d** (22%). These results are consistent with an electrophilic cyclonickelation mechanism for this family of phosphinite ligands. A similar trend (OMe > Me > CO₂Me) was also found for the impact of the 4-R substituent in the nickelation of resorcinol-based bis(phosphinite) ligands to give the corresponding POCOP-type pincer complexes of Ni(II).²⁶

The new complexes **2b–d** and **3b–d** generated in the course of the above study were characterized by comparing their NMR spectral patterns to those of their analogues **2a** and **3a**. For example, similarly to what was observed for **2a**, a broad ³¹P singlet was detected for **2b,c** (136 ppm) and for **2d** (131 ppm), whereas AB doublets featuring large ²J_{PP} values were observed in the ³¹P{¹H} NMR spectra of **3b–d** (~152 and 185 ppm; ²J_{PP} ≈ 325 Hz). Single crystals were also grown for **2b–d** and subjected to X-ray diffraction studies. Figure 3 shows structure diagrams for **2a,c**, and Table 1 gives selected structural parameters for **2a–d** (see Figure S6 in the Supporting Information for structure diagrams of **2b,d**). Complexes **2a,b** display an inversion center at the Ni atom, and a nearly ideal square-planar geometry is seen for **2a,b,d**, whereas **2c** shows an unexpectedly large distortion in the Br–Ni–Br angle (166°). The Ni–P and Ni–Br distances in **2a–d**, 2.22–2.24 and 2.29–2.30 Å, respectively, are somewhat shorter than the corresponding distances in **3a** (2.25 and 2.37 Å).

Question of Site Selectivity in Cyclonickelation. The cyclometalation reactions discussed to this point have involved phosphinite ligands derived from either phenol or its para-substituted derivatives, all of which can give only one product of monometalation. The same scenario should normally hold for ortho-substituted analogues, whereas R₂POAr derived from meta-substituted arenols 3-R'-C₆H₄OH can, in principle, result in two different cyclonickelation products depending on which C–H is metalated: that situated between the OPR₂ and R' or that situated ortho to the OPR₂ and para to R'. We have addressed this question briefly by studying the cyclonickelation of 3-fluorophenol, as described below. The choice of F as substituent was predicated by its similar steric properties relative to H, which should ensure that electronic effects are the dominant factor in site selectivity.

The ligand 3-F-C₆H₄OP(*i*-Pr)₂ (**1e**) was prepared similarly to **1a–d** described above and was treated with $[(i\text{-PrCN})NiBr_2]_n$ and NEt₃ (0.5 and 1.2 equiv, respectively) at 100 °C in toluene for 25 h (Scheme 5). ³¹P{¹H} NMR analysis of the reaction mixture at $t = 25$ h showed the emergence of two sets of AB resonances assigned to the cyclonickelated species analogous to **3a** (Figure S7, Supporting Information). The major resonances appeared at 155.5 and 186.5 ppm ($J_{PP} = 325$ Hz) and have been assigned to isomer **3e_p**, wherein the nickelated carbon atom is para to F. The minor AB resonances (²J_{PP} = 341 Hz) appearing at ca. 184 ppm (⁴J_{PF} = 2 Hz) and ca. 156 ppm (⁴J_{PF} = 32 Hz) have been assigned to the isomer **3e_o**, wherein the nickelated carbon atom is ortho to F.

In addition to the AB resonances noted above, the spectrum shows two broad singlets assigned to the free ligand **1e** (150 ppm) and to the bis(phosphinite) species *trans*-{3-F-C₆H₄OP(*i*-Pr)₂}₂NiBr₂ (**2e**) (139 ppm); the presence of these signals indicates that the C–H nickelation reaction is incomplete. The ¹⁹F NMR analysis of the final mixture confirmed the presence of four F-bearing species, and integration of ¹⁹F and ³¹P{¹H} signals indicated ~65% cyclonickelation and a 5.6:1 ratio for the cyclonickelation products **3e_p** and **3e_o**. The greater preference for metalation of the C–H moiety para to F in 3-F-C₆H₄OP(*i*-Pr)₂ parallels the 6:1 selectivity reported for Pd-catalyzed acetoxylation of 2-(3-fluorophenyl)pyridine at the position para to F.²⁷

Ortho Derivatization. As mentioned earlier, a number of metallacyclic complexes of nickel have been prepared by oxidative addition of C–X moieties to zerovalent Ni precursors.^{10–13} It is also known that the Ni–Ar moiety in

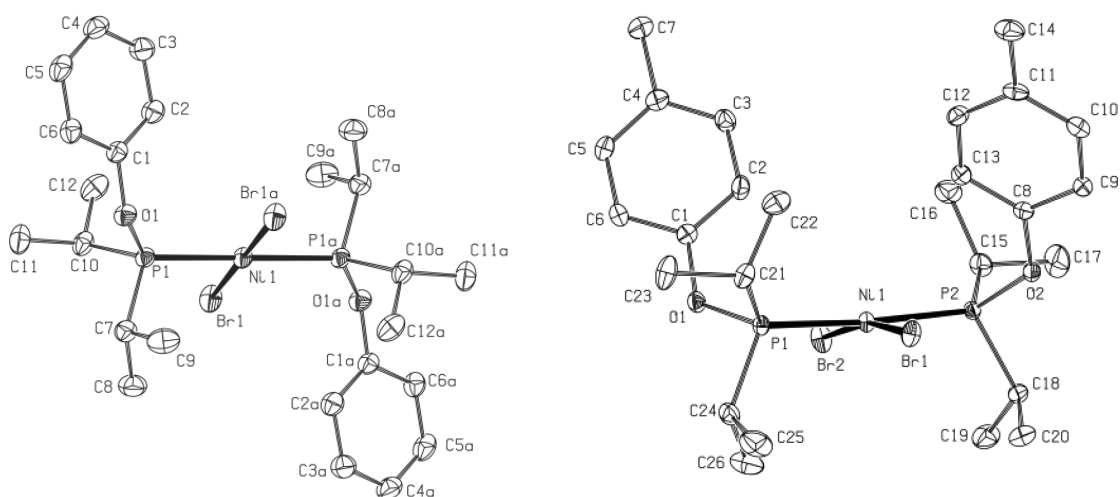


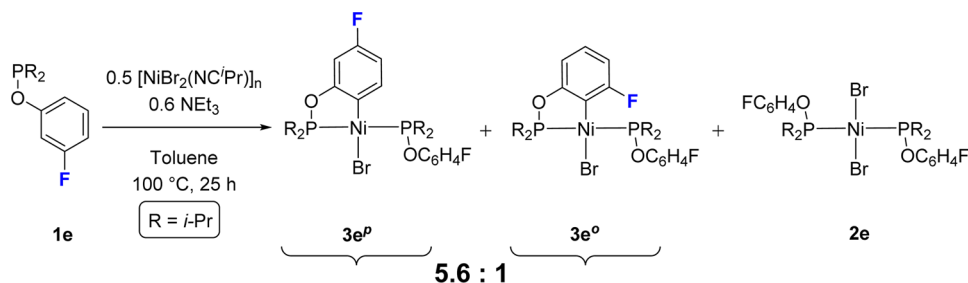
Figure 3. Structure diagrams for complexes **2a** (left) and **2c** (right). Thermal ellipsoids are shown at the 50% probability level, and hydrogen atoms are omitted for clarity. Selected structural parameters are given in Table 1.

Table 1. Selected Bond Distances (Å) and Angles (deg) for Complexes **2a–d**

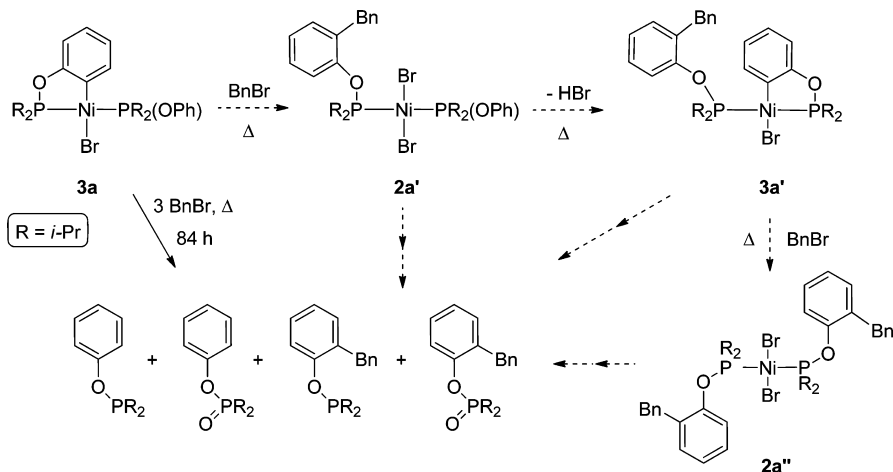
compd	Ni–P1	Ni–P2	Ni–Br1	Ni–Br2	P–Ni–P	Br–Ni–Br	P1–Ni–Br1
2a	2.243(1)		2.297(1)		180.0	180.0	88.81(1)
2b^a	2.238(1)		2.298(1)		180.0	180.0	88.60(2)
2c	2.225(1)	2.240(1)	2.303(1)	2.301(1)	175.90(2)	166.63(1)	87.23(1)
2d^a	2.230(1)	2.228(1)	2.290(1)	2.292(1)	179.83(2)	179.79(2)	89.16(2)

^aValues given are for molecule 1.

Scheme 5. Cyclonickelation of **1e**



Scheme 6. Postulated Pathways for Benzylation of **3a**



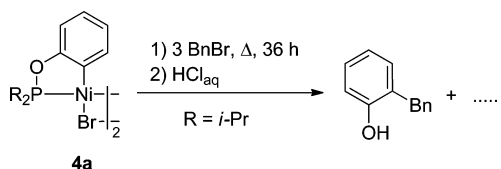
some of these complexes is fairly reactive, undergoing insertion of CO, SO₂, or alkynes²⁸ or initiating polymerization of olefins.²⁹ We have briefly investigated the reactivity of the

newly created C–Ni bonds in the cyclometalated complexes **3a** and **4a** to establish the feasibility of developing a viable methodology for functionalizing arenols.³⁰

The first tests were done using complex **3a**, as follows. A J. Young NMR tube containing an equimolar mixture of **3a** and benzyl bromide in 0.5 mL of toluene (0.08 M) was heated to 100 °C for 84 h, and the final mixture was subjected to $^{31}\text{P}\{^1\text{H}\}$ NMR and GC/MS analysis. The NMR analysis confirmed the complete consumption of **3a**, and GC/MS showed the presence of the starting ligand **1a** (m/z 210), its benzylated derivative **1a-Bn** (m/z 300), and the oxidized forms of these phosphinites (m/z 226 and 316, respectively). Interestingly, the ratio of benzylated to nonbenzylated fractions was greater than 1:1 (~1.25:1.0), which implies that the putative bis-(phosphinite) species formed as a result of the initial benzylation reacts further to cyclometalate the monodentate phosphinite moiety, as shown in Scheme 6 (species **3a'** and **2a''**). It should be emphasized that we have no evidence for the formation of products featuring benzylation at *both* ortho sites.

The benzylation reaction was also conducted with the dimeric species **4a**, which has a 1:1 ratio of Ni to phosphinite (3 equiv of benzyl bromide; toluene, 90 °C; 36 h). The final reaction mixture was subjected to a hydrolytic workup in the presence of HCl_{aq} , followed by column chromatography (SiO_2) to give 2-benzylphenol in 47% isolated yield (Scheme 7). The

Scheme 7. Benzylation of **4a**



identity of this product was confirmed by GC/MS (m/z 184) and by ^1H and ^{13}C NMR (e.g., a singlet at 3.91 ppm corresponding to the CH_2Ph proton and a deshielded singlet at 4.83 ppm for OH). These results demonstrate the feasibility of Ni-promoted ortho functionalization of phenol through its $i\text{-Pr}_2\text{P}$ phosphinite derivative.

Monitoring the reaction of **4a** with PhCH_2Br by $^{31}\text{P}\{^1\text{H}\}$ NMR spectroscopy provided further support for the pathway(s) postulated in Scheme 6. Thus, we observed that over time the signal due to **4a** (s, 199 ppm) was replaced by two broad singlets at 134 and 133 ppm, which can be assigned to species **2a'** and **2a''** shown in Scheme 6, and three pairs of AB doublets ($^2J_{\text{PP}} = 324$ Hz) at ca. 183 and ca. 149–151 ppm. Of these, the more intense set of signals at 183.4 and 149.3 ppm is tentatively assigned to **3a'**, while the less intense sets are likely due to closely related products bearing different OAr moieties.

CONCLUSION

The results reported above establish that it is feasible to ortho nickelate the aryl phosphinites $i\text{-Pr}_2\text{P}(\text{OAr})$ using a simple Ni(II) precursor. The isolation and full characterization of the two nickelacycle compounds **3a** and **4a** has allowed us to study their structural and spectroscopic properties. We have also determined the conditions favoring the formation of one or the other of these complexes and investigated the importance of aryl substituents on the C–H nickelation pathway ($\text{OMe} > \text{Me} > \text{COOMe}$). The latter studies point to an electrophilic C–H nickelation taking place with a mono(phosphinite) intermediate generated in situ through ligand dissociation. Our observations also indicate that phosphinite dissociation favors the C–H nickelation process.

Ortho nickelation of 3-F- $\text{C}_6\text{H}_4\text{OP}(i\text{-Pr})_2$ allowed us to establish that nickelation is favored at the C–H moiety para with respect to the fluoro substituent. Further studies are needed to determine the site selectivity of C–H nickelation with other substituents. Benzylation of the ipso-C atoms in **3a** and **4a** with benzyl bromide provided proof of concept for the feasibility of the envisaged areneol functionalization strategy, but much work remains to be done to expand the scope of functionalization and to identify reaction conditions under which the process can be catalytic in both Ni and chlorophosphine.

EXPERIMENTAL SECTION

General Considerations. Unless otherwise indicated, all manipulations were carried out under a nitrogen atmosphere using standard Schlenk techniques and an inert-atmosphere box. Solvents were dried by passage over activated alumina, collected under nitrogen, and stored over 4 Å molecular sieves. Triethylamine was dried by distillation over CaH_2 . The synthesis and characterization of ligands **1a,c** has been reported by Bedford et al.;¹⁸ a slightly modified version of this procedure, described below, was used to prepare **1b,d,e**. Synthesis of the nickel precursor $[(i\text{-PrCN})\text{NiBr}_2]_n$ used throughout this study has been described previously.¹⁹ All other reagents were purchased from Sigma-Aldrich and were used without further purification.

The NMR spectra were recorded at 400 or 500 MHz (^1H), 100.56 MHz (^{13}C), and 161.9 MHz (^{31}P). Chemical shift values are reported in ppm (δ) and referenced internally to the residual solvent signals (^1H and ^{13}C : 7.26 and 77.16 ppm for CDCl_3 ; 7.16 and 128.06 ppm for C_6D_6 ; 5.32 and 53.84 ppm for CD_2Cl_2) or externally (^{31}P , H_3PO_4 in D_2O , δ 0); J values are given in Hz. The elemental analyses were performed by the Laboratoire d'Analyse Élémentaire, Département de chimie, Université de Montréal.

(3-F- $\text{C}_6\text{H}_4\text{O}$)P($i\text{-Pr}$)₂ (1e**).** Dropwise addition of $\text{ClP}(i\text{-Pr})_2$ (490 μL , 3.0 mmol) to a solution of 3-fluorophenol (271 μL , 3.0 mmol) and NEt_3 (460 μL , 3.5 mmol) in THF (25 mL) led to the appearance of a white precipitate. The reaction mixture was stirred at room temperature for 1 h and evaporated, and the solid residues were extracted with hexane (2×25 mL). Evaporation under vacuum gave the crude product as a colorless oil (543 mg, 78%), which was shown to be greater than 98% pure by NMR spectroscopy. This material was used without further purification in subsequent experiments. ^1H NMR (400 MHz, 20 °C, C_6D_6): δ 0.91 (dd, $J_{\text{HP}} = 15.90$, $J_{\text{HH}} = 7.23$, 6H, $\text{CH}(\text{CH}_3)_2$), 1.06 (dd, $J_{\text{HP}} = 10.65$, $J_{\text{HH}} = 7.0$, 6H, $\text{CH}(\text{CH}_3)_2$), 1.71 (hd, $J_{\text{HH}} = 7.08$, $J_{\text{HP}} = 2.75$, 2H, $\text{PCH}(\text{CH}_3)_2$), 6.51 (m, 1H, H_{Ar}), 6.85 (m, 1H, H_{Ar}), 6.92 (m, 1H, H_{Ar}), 7.03 (m, 1H, H_{Ar}). ^{19}F NMR (376 MHz, 20 °C, C_6D_6): δ -111.56 (m). $^{31}\text{P}\{^1\text{H}\}$ NMR (162 MHz, 20 °C, CDCl_3): δ 151.14 (s). $^{13}\text{C}\{^1\text{H}\}$ NMR (101 MHz, 20 °C, CDCl_3): δ 17.03 (d, $J_{\text{CP}} = 8.56$, 2C, CH_3), 17.71 (d, $J_{\text{CP}} = 20.5$, 2C, CH_3), 28.52 (d, $J_{\text{CP}} = 18.42$, 2C, $\text{PCH}(\text{CH}_3)_2$), 106.48 (dd, $J_{\text{FC}} = 24.08$, $J_{\text{PC}} = 11.50$, 1C, CH_{Ar}), 108.71 (d, $J_{\text{FC}} = 21.26$, 1C, CH_{Ar}), 114.50 (dd, $J_{\text{FC}} = 2.97$, $J_{\text{PC}} = 11.0$, 1C, CH_{Ar}), 130.47 (d, $J_{\text{FC}} = 9.98$, 1C, CH_{Ar}), 161.35 (vt, $J_{\text{PC}} = J_{\text{FC}} = 10.45$, 1C, $\text{C}_{\text{Ar}}\text{OP}$), 163.99 (d, $J_{\text{FC}} = 245.6$, 1C, F-C_{Ar}). Anal. Calcd for $\text{C}_{12}\text{H}_{18}\text{FOP}$ (228.24): C, 63.15; H, 7.95. Found: C, 63.43; H, 8.20.

(4-OMe- $\text{C}_6\text{H}_4\text{O}$)P($i\text{-Pr}$)₂ (1b**).** The procedure described above for the preparation of **1e** was used here to give **1b** as a colorless oil (1.87 g, 97%). ^1H NMR (400 MHz, 20 °C, CDCl_3): δ 1.13 (dd, $J_{\text{HP}} = 15.80$, $J_{\text{HH}} = 7.25$, 6H, $\text{CH}(\text{CH}_3)_2$), 1.21 (dd, $J_{\text{HP}} = 10.70$, $J_{\text{HH}} = 6.98$, 6H, $\text{CH}(\text{CH}_3)_2$), 1.92 (hd, $J_{\text{HH}} = 7.09$, $J_{\text{HP}} = 2.17$, 2H, $\text{PCH}(\text{CH}_3)_2$), 3.74 (s, 3H, OMe), 6.81 (d, $J_{\text{HH}} = 6.80$, 2H, H_{Ar}), 7.05 (dd, $J_{\text{HH}} = 8.70$, $J_{\text{PH}} = 1.56$, 2H, H_{Ar}). $^{31}\text{P}\{^1\text{H}\}$ NMR (162 MHz, 20 °C, CDCl_3): δ 150.6 (s). $^{13}\text{C}\{^1\text{H}\}$ NMR (101 MHz, 20 °C, CDCl_3): δ 16.97 (dd, $J_{\text{CP}} = 8.53$, 2C, CH_3), 17.74 (d, $J_{\text{CP}} = 20.27$, 2C, CH_3), 28.26 (d, $J_{\text{CP}} = 17.86$, 2C, $\text{PCH}(\text{CH}_3)_2$), 55.40 (s, 1C, OMe), 114.31 (s, 2C, CH_{Ar}), 119.25 (d, $J_{\text{PC}} = 9.53$, 2C, CH_{Ar}), 153.21 (d, $J_{\text{PC}} = 8.86$, 1C, C_{Ar}), 154.36 (s, 1C, C_{Ar}). Anal. Calcd for $\text{C}_{13}\text{H}_{21}\text{O}_2\text{P}$ (240.28): C, 64.98; H, 8.81. Found: C, 64.90; H, 8.94.

(4-COOMe-C₆H₄O)P(*i*-Pr)₂ (1d). The procedure described above for the preparation of **1e** was used here to give **1d** as a colorless oil (0.90 g, 87%). ¹H NMR (400 MHz, 20 °C, CDCl₃): δ 1.04–1.09 (m, 6H, CH(CH₃)₂), 1.11–1.15 (m, 6H, CH(CH₃)₂), 1.92 (m, 2H, PCH(CH₃)₂), 3.85 (m, 3H, OMe), 7.13 (m, 2H, H_{Ar}), 7.94 (m, 2H, H_{Ar}). ³¹P{¹H} NMR (162 MHz, 20 °C, CDCl₃): δ 150.4 (s). ¹³C{¹H} NMR (101 MHz, 20 °C, CDCl₃): δ 17.01 (d, J_{CP} = 8.32, 2C, CH₃), 17.71 (d, J_{CP} = 20.20, 2C, CH₃), 28.37 (d, J_{CP} = 17.81, 2C, PCH(CH₃)₂), 51.90 (s, 1C, OMe), 118.15 (d, J_{PC} = 11.13, 2C, CH_{Ar}), 123.40 (s, 1C, C_{Ar}), 131.5 (s, 2C, CH_{Ar}), 163.48 (d, J_{PC} = 8.42, 1C, C=O or C_{Ar}OP), 166.84 (s, 1C, C=O or C_{Ar}OP). Anal. Calcd for C₁₄H₂₁O₃P (268.29): C, 62.67; H, 7.89. Found: C, 62.59; H, 7.91.

trans-*i*-Pr₂P(OPh)₂NiBr₂ (2a). [(*i*-PrCN)NiBr₂]_n (1.9 mmol, 547 mg) was added to a solution of **1a** (3.81 mmol, 800 mg) in toluene (5 mL), and the resulting brown solution was stirred for 2 h at room temperature. Filtration and evaporation gave the target compound as a dark brown solid (995 mg, 82%). Brown single crystals were obtained through slow crystallization in toluene (2 days at –37 °C). This complex is fairly air stable over short periods, but aerobic decomposition sets in after 1 week to give an NMR-silent beige powder. ¹H NMR (500 MHz, 20 °C, CD₂Cl₂): δ 1.42 (d, J_{HH} = 7.15, 12H, CH(CH₃)), 1.54 (d, J_{HH} = 7.29, 12H, CH(CH₃)), 2.79 (h, J_{HH} = 7.19, 4H, CH(CH₃)), 7.11 (tt, J_{HH} = 7.15, J_{HH} = 1.02, 2H, H_{para}), 7.37 (dd, J_{HH} = 8.64, J_{HH} = 7.41, 4H, H_{meta}), 7.66 (dm, J_{HH} = 7.69, 4H, H_{ortho}). ¹H NMR (500 MHz, –68 °C, CD₂Cl₂): δ 1.37 (dt', J_{HH} = 7.25, J_{HP} = 7.17, 12H, CH(CH₃)), 1.47 (dt', J_{HH} = 7.83, J_{HP} = 7.75, 12H, CH(CH₃)), 2.70 (m, 4H, CH(CH₃)), 7.10 (t, J_{HH} = 7.37, 2H, H_{para}), 7.37 (dd, J_{HH} = 8.3, J_{HH} = 7.66, 4H, H_{meta}), 7.66 (d, J_{HH} = 8.01, 4H, H_{ortho}). ¹³C{¹H} NMR (125 MHz, 20 °C, CD₂Cl₂): δ 18.25 (s, 4C, CH₃), 19.70 (s, 4C, CH₃), 30.08 (s, 4C, PCH(CH₃)₂), 120.23 (s, 4C, CH_{Ar}), 122.96 (s, 2C, CH_{Ar}), 129.30 (s, 4C, CH_{Ar}), 155.28 (s, 2C, C_{Ar}OP). ¹³C{¹H} NMR (125 MHz, –68 °C, CD₂Cl₂): δ 17.63 (s, 4C, CH₃), 19.12 (s, 4C, CH₃), 29.03 (vt, J_{PC} = 11.95, 4C, PCH(CH₃)₂), 119.20 (s, 4C, CH_{Ar}), 122.26 (s, 2C, CH_{Ar}), 128.80 (s, 4C, CH_{Ar}), 154.26 (s, 1C, C_{Ar}OP). ³¹P{¹H} NMR (201 MHz, 20 °C, CD₂Cl₂): δ 135.8 (bs, 1P). ³¹P{¹H} NMR (201 MHz, –68 °C, CD₂Cl₂): δ 136.2 (s, 1P). Anal. Calcd for C₂₄H₃₈Br₂NiO₂P₂ (639.01): C, 45.11; H, 5.99. Found: C, 45.19; H, 5.92.

trans-*i*-Pr₂P(4-Ome-C₆H₄O)₂NiBr₂ (2b). The procedure described above for the preparation of **2a** was used to give **2b** as a dark orange solid (458 mg, 80%). ¹H NMR (400 MHz, 20 °C, CDCl₃): δ 1.42 (m, 24H, CH(CH₃)), 2.81 (m, 4H, CH(CH₃)), 3.82 (s, 6H, OMe), 6.88 (m, 4H, H_{Ar}), 7.51 (m, 4H, H_{Ar}). ¹³C{¹H} NMR (101 MHz, 20 °C, CDCl₃): δ 18.13 (s, 4C, CH₃), 19.43 (s, 4C, CH₃), 29.73 (s, 4C, PCH(CH₃)₂), 55.63 (s, 2C, OMe), 114.02 (s, 4C, CH_{Ar}), 120.82 (s, 4C, CH_{Ar}), 148.73 (s, 2C, OC_{Ar}), 155.07 (s, 2C, C_{Ar}OP). ³¹P{¹H} NMR (162 MHz, 20 °C, CDCl₃): δ 136.0 (bs, 1P). Anal. Calcd for C₂₆H₄₂Br₂NiO₄P₂ (699.06): C, 44.67; H, 6.06. Found: C, 44.71; H, 6.14.

trans-*i*-Pr₂P(4-Me-C₆H₄O)₂NiBr₂ (2c). The procedure described above for the preparation of **2a** was used to give **2c** as a dark orange solid (800 mg, 80%). ¹H NMR (400 MHz, 20 °C, CDCl₃): δ 1.40 (d, J_{HH} = 7.06, 12H, CH(CH₃)), 1.52 (d, J_{HH} = 7.19, 12H, CH(CH₃)), 2.33 (s, 6H, Me), 2.75 (h, J_{HH} = 7.12, 4H, CH(CH₃)), 7.11 (d, J_{HH} = 8.19, 4H, H_{Ar}), 7.50 (d, J_{HH} = 8.39, 4H, H_{ortho}). ³¹P{¹H} NMR (162 MHz, 20 °C, CDCl₃): δ 136.0 (bs, 1P). Anal. Calcd for C₂₆H₄₂Br₂NiO₂P₂ (667.06): C, 46.81; H, 6.35. Found: C, 47.08; H, 6.44.

trans-*i*-Pr₂P(4-COOMe-C₆H₄O)₂NiBr₂ (2d). The procedure described above for the preparation of **2a** was used to give **2d** as a dark orange solid (504 mg, 91%). ¹H NMR (300 MHz, 20 °C, CDCl₃): δ 1.40 (d, J_{HH} = 6.43, 12H, CH(CH₃)), 1.55 (d, J_{HH} = 6.41, 12H, CH(CH₃)), 2.76 (h, J_{HH} = 7.13, 4H, CH(CH₃)), 3.92 (s, 6H, OMe), 7.63 (d, J_{HH} = 7.63, 4H, H_{Ar}), 8.04 (d, J_{HH} = 8.67, 4H, H_{ortho}). ¹³C{¹H} NMR (75 MHz, 20 °C, CDCl₃): δ 18.20 (s, 4C, CH₃), 19.70 (s, 4C, CH₃), 29.90 (s, 4C, PCH(CH₃)₂), 52.16 (s, 2C, OMe), 119.83 (s, 4C, CH_{Ar}), 124.76 (s, 2C, C_{Ar}), 131.09 (s, 4C, CH_{Ar}), 158.86 (s, 2C, C_{Ar}OP), 166.71 (s, 2C, C=O). ³¹P{¹H} NMR (162 MHz, 20 °C, CDCl₃): δ 139.9 (bs, 1P). Anal. Calcd for C₂₈H₄₂Br₂NiO₃P₂ (847.22): C, 49.62; H, 5.95. Found: C, 49.28; H, 5.89.

trans-(κ²P,C-*i*-Pr₂POPh)(*i*-Pr₂POPh)NiBr (3a). [(*i*-PrCN)NiBr₂]_n (1.25 mmol, 360 mg) and NEt₃ (1.66 mmol, 232 μL) were added to a solution of **1a** (500 mg, 2.08 mmol) in toluene (20 mL). The resulting brown solution was stirred over 48 h at 100 °C and evaporated, and the solid residues were extracted with toluene (2 × 30 mL). Evaporation of the combined extracts gave **3a** as a yellow solid (540 mg, 93%), which was found to be greater than 98% pure by NMR spectroscopy; this material was used in subsequent experiments without further purification. Single crystals were obtained from a saturated hexane solution at –37 °C. ¹H NMR (400 MHz, 20 °C, C₆D₆): δ 1.27 (vt, J_{HP} = J_{HH} = 6.35, 6H, CH(CH₃)₂), 1.30 (dd, J_{HP} = 4.56, J_{HH} = 7.03, 6H, CH(CH₃)₂), 1.51 (dd, J_{HP} = 16.84, J_{HH} = 7.21, 6H, CH(CH₃)₂), 1.56 (dd, J_{HP} = 16.03, J_{HH} = 7.35, 6H, CH(CH₃)₂), 2.49 (m, 2H, PCH(CH₃)₂), 2.81 (m, 2H, PCH(CH₃)₂), 6.51 (t, J_{HH} = 7.47, 1H, H_{Ar}), 6.67 (t, J_{HH} = 7.40, 1H, H_{Ar}), 6.80–6.87 (m, 2H, H_{Ar}), 6.93 (t, J_{HH} = 7.65, 2H, H_{Ar}), 7.57 (d, J_{HH} = 8.49, 2H, H_{Ar}), 7.64 (d, J_{HH} = 7.76, 1H, H_{Ar}). ¹³C{¹H} NMR (101 MHz, 20 °C, CDCl₃): δ 17.12 (s, 2C, CH₃), 17.87 (s, 2C, CH₃), 18.79 (d, J_{CP} = 3.58, 2C, CH₃), 20.52 (d, J_{CP} = 4.68, 2C, CH₃), 28.63 (dd, J_{CP} = 2.47, J_{CP} = 23.79, 2C, PCH(CH₃)₂), 29.94 (dd, J_{CP} = 2.82, J_{CP} = 17.61, 2C, PCH(CH₃)₂), 110.35 (d, J_{PC} = 13.53, 1C, CH_{Ar}), 120.0 (d, J_{CP} = 6.14, 2C, CH_{Ar}), 120.55 (m, 1C, CH_{Ar}), 122.51 (s, CH_{Ar}), 126.46 (s, 1C, CH_{Ar}), 128.91 (s, 2C, CH_{Ar}), 132.0 (dd, J_{CP} = 14.30, J_{CP} = 29.37, 1C, Ni-C_{Ar}), 142.25 (d, J_{CP} = 11.04, 1C, CH_{Ar}), 154.73 (d, J_{CP} = 4.62, 1C, OC_{Ar}), 168.38 (dd, J_{CP} = 4.33, J_{CP} = 16.24, 1C, OC_{Ar}). ³¹P{¹H} NMR (162 MHz, 20 °C, C₆D₆): δ 151.86 (d (AB), J_{PP} = 325, 1P), 184.66 (d (AB), J_{PP} = 325, 1P). Anal. Calcd for C₂₄H₃₇BrNiO₂P₂ (558.09): C, 51.65; H, 6.68. Found: C, 51.94; H, 6.71.

[(κ²P,C-*i*-Pr₂POPh)NiBr(μ-Br)]₂ (4a). [(*i*-PrCN)NiBr₂]_n (5.45 g, 19 mmol) and NEt₃ (2.64 mL, 19 mmol) were added to a solution of **1a** (2 g, 9.5 mmol) in toluene (50 mL). The resulting brown solution was stirred over 40 h at 100 °C to give a green mixture, which was evaporated, and the solid residues were extracted with toluene (2 × 50 mL). The extracted solution was once again evaporated to dryness and washed with hexane (25 mL) to give **4a** as a yellow powder (2.3 g, 70%). Single crystals were obtained from a saturated toluene/hexane solution at –37 °C. ¹H NMR (500 MHz, 20 °C, CD₂Cl₂): δ 1.37 (dd, J_{HH} = 6.80, J_{HP} = 14.60, 24H, CH(CH₃)), 1.57 (dd, J_{HH} = 6.00, J_{HP} = 17.37, 24H, CH(CH₃)), 2.35 (m, 4H, CH(CH₃)), 6.59 (m, 4H, H_{Ar}), 6.92 (m, 2H, H_{Ar}), 7.27 (m, 2H, H_{Ar}). ¹³C{¹H} NMR (125 MHz, 20 °C, CD₂Cl₂): δ 16.69 (s, 4C, CH₃), 18.00 (s, 4C, CH₃), 28.90 (d, J_{CP} = 26.60, 4C, PCH(CH₃)₂), 110.23 (d, J_{CP} = 13.88, 2C, CH_{Ar}), 121.02 (s, 2C, CH_{Ar}), 126.95 (s, 2C, CH_{Ar}), 128.56 (bm, 2C, NiC_{Ar}), 140.71 (s, 2C, CH_{Ar}), 166.58 (d, J_{CP} = 12.02, 2C, OC_{Ar}). ³¹P{¹H} NMR (201 MHz, 20 °C, CD₂Cl₂): δ 199.1 (s, 1P). Anal. Calcd for C₂₄H₃₆Br₂Ni₂O₂P₂ (695.68): C, 41.44; H, 5.22. Found: C, 42.06; H, 5.22.

Functionalization of Phenol to 2-Benzylphenol. Benzyl bromide (2.84 mmol, 338 μL) was added to a solution of **4a** (0.95 mmol, 660 mg) in toluene (25 mL), and the resulting mixture was stirred for 36 h at 90 °C. The final mixture was added to HCl_{aq} (100 mL, 2.5 M) and extracted with CH₂Cl₂ (3 × 50 mL). The combined organic phases were dried over MgSO₄, filtered, and evaporated under vacuum, and the residue obtained was purified on a silica gel column (CHCl₃/hexane 1/1) to give 2-benzylphenol (R_f = 0.1) as a white solid (47%, 164 mg). ¹H NMR (400 MHz, 20 °C, CDCl₃): δ 3.91 (s, 2H, CH₂), 4.83 (s, 1H, OH), 6.63 (d, J_{HH} = 7.81, 1H, CH_{Ar}), 6.82 (t, J_{HH} = 7.14, 1H, CH_{Ar}), 7.03 (m, 2H, CH_{Ar}), 7.14–7.21 (m, 5H, CH_{Ar}). ¹³C NMR (125 MHz, 20 °C, CDCl₃): δ 36.31 (s, 1C, CH₂), 115.80 (s, 1C, CH_{Ar}), 121.06 (s, 1C, CH_{Ar}), 126.38 (s, 1C, CH_{Ar}), 127.18 (s, 1C, C_q), 127.86 (s, 1C, CH_{Ar}), 128.68 (s, 2C, CH_{Ar}), 128.80 (s, 2C, CH_{Ar}), 131.04 (s, 1C, CH_{Ar}), 140.03 (s, 1C, C_q), 153.66 (s, 1C, C_q). GC-MS: m/z 184 (M⁺).

Crystal Structure Determinations. The crystallographic data for compounds **2a,e** and **3a** were collected on a Bruker Microstar generator (micro source) equipped with Helios optics, a Kappa Nonius goniometer, and a Platinum135 detector. The crystallographic data for complexes **4a** and **2c,d** were collected on a Bruker APEX II instrument equipped with an Incoatec I μ S Microsource and a Quazar MX monochromator. Cell refinement and data reduction were done

using SAINT.³¹ An empirical absorption correction, based on the multiple measurements of equivalent reflections, was applied using the program SADABS.³² The space group was confirmed by the XPREP routine³³ in the program SHELXTL.³⁴ The structures were solved by direct methods and refined by full-matrix least squares and difference Fourier techniques with SHELXL-97.³⁵ All non-hydrogen atoms were refined with anisotropic displacement parameters. Hydrogen atoms were set in calculated positions and refined as riding atoms with a common thermal parameter.

■ ASSOCIATED CONTENT

Supporting Information

Tables, figures, and CIF files giving crystal data and collection/refinement parameters, structural diagrams for complexes **2b,d**, various NMR spectra, and crystallographic data. This material is available free of charge via the Internet at <http://pubs.acs.org>. Complete details of the X-ray analyses reported herein have also been deposited at The Cambridge Crystallographic Data Centre (CCDC 1012836 (**2a**), 1012835 (**2c**), 1012832 (**2d**), 1012834 (**2e**), 1012833 (**3a**), 1012831 (**4a**)). These data can be obtained free of charge via www.ccdc.cam.ac.uk/data_request/cif, by emailing data_request@ccdc.cam.ac.uk, or by contacting The Cambridge Crystallographic Data Centre, 12, Union Road, Cambridge CB2 1EZ, U.K. (fax +44 1223 336033).

■ AUTHOR INFORMATION

Corresponding Author

*E-mail for D.Z.: zargarian.davit@umontreal.ca.

Notes

The authors declare no competing financial interest.

■ ACKNOWLEDGMENTS

The authors are grateful to the NSERC of Canada for a Discovery Grant to D.Z., the Université de Montréal, Centre in Green Chemistry and Catalysis, and FQRNT for graduate fellowships to B.V., and Dr. Michel Simard for his valuable assistance with crystallography.

■ REFERENCES

- (1) For recent reviews on the subject of C–H functionalization see: (a) Kakiuchi, F.; Kochi, T. *Synthesis* **2008**, 2008, 3013. (b) Ackermann, L. *Chem. Rev.* **2011**, *111*, 1315. (c) Yamaguchi, J.; Yamaguchi, A. D.; Itami, K. *Angew. Chem., Int. Ed.* **2012**, *51*, 8960. (d) Ackermann, L. *Chem. Commun.* **2010**, 46, 4866. (e) Chen, D. Y.-K.; Youn, S. W. *Chem. Eur. J.* **2012**, *18*, 9452.
- (2) For a recent review of Ru-based C–H functionalizations see: Arockiam, P. B.; Bruneau, C.; Dixneuf, P. H. *Chem. Rev.* **2012**, *112*, 5879.
- (3) For recent reviews of Rh- and Ir- based C–H functionalization methods see: (a) Klei, S. R.; Tan, K. L.; Golden, J. T.; Yung, C. M.; Thalji, R. K.; Ahrendt, K. A.; Ellman, J. A.; Tilley, T. D.; Bergman, R. G. C–H Bond Activation by Iridium and Rhodium Complexes: Catalytic Hydrogen–Deuterium Exchange and C–C Bond-Forming Reactions. In *Activation and Functionalization of C–H Bonds*; Goldberg, K. I., Goldman, A. S., Eds.; American Chemical Society: Washington, DC, 2004; ACS Symposium Series 885, pp 46–55. (b) Colby, D. A.; Bergman, R. G.; Ellman, J. A. *Chem. Rev.* **2010**, *110*, 624. (c) Rouquet, G.; Chatani, N. *Angew. Chem., Int. Ed.* **2013**, *52*, 11726.
- (4) For recent reviews of Pd-based C–H functionalizations see: (a) Lyons, T. W.; Sanford, M. S. *Chem. Rev.* **2010**, *110*, 1147. (b) Xu, L.-M.; Li, B.-J.; Yang, Z.; Shi, Z.-J. *Chem. Soc. Rev.* **2010**, *39*, 712. (c) Sehnal, P.; Taylor, R. J. K.; Fairlamb, I. J. S. *Chem. Rev.* **2010**, *110*, 824.

- (5) (a) Yoshikai, N.; Matsumoto, A.; Norinder, J.; Nakamura, E. *Angew. Chem., Int. Ed.* **2009**, *48*, 2925. (b) Norinder, J.; Matsumoto, A.; Yoshikai, N.; Nakamura, E. *J. Am. Chem. Soc.* **2008**, *130*, 5858. (c) Wen, J.; Zhang, J.; Chen, S.-Y.; Li, J.; Yu, X.-Q. *Angew. Chem., Int. Ed.* **2008**, *47*, 8897. (d) Liu, W.; Cao, H.; Lei, A. *Angew. Chem., Int. Ed.* **2010**, *49*, 2004.
- (6) (a) Yoshikai, N. *Synlett* **2011**, 8, 1047. (b) Gao, K.; Yoshikai, N. *Chem. Commun.* **2012**, 48, 4305. (c) Lee, P.-S.; Fujita, T.; Yoshikai, N. *J. Am. Chem. Soc.* **2011**, *133*, 17283. (d) Gao, K.; Yoshikai, N. *J. Am. Chem. Soc.* **2013**, *135*, 9279. (e) Gao, K.; Yoshikai, N. *J. Am. Chem. Soc.* **2011**, *133*, 400. (f) Gao, K.; Lee, P.-S.; Fujita, T.; Yoshikai, N. *J. Am. Chem. Soc.* **2010**, *132*, 12249.
- (7) (a) Shacklady-McAtee, D. M.; Dasgupta, S.; Watson, M. P. *Org. Lett.* **2011**, *13*, 3490. (b) Ogata, K.; Atsumi, Y.; Shimada, D.; Fukuzawa, S. *Angew. Chem., Int. Ed.* **2011**, *50*, 5896. (c) Shiota, H.; Ano, Y.; Aihara, Y.; Fukumoto, Y.; Chatani, N. *J. Am. Chem. Soc.* **2011**, *133*, 14952. (d) Kanyiva, K. S.; Nakao, Y.; Hiyama, T. *Angew. Chem., Int. Ed.* **2007**, *46*, 8872. (e) Nakao, Y.; Kanyiva, K. S.; Hiyama, T. *J. Am. Chem. Soc.* **2008**, *130*, 2448. (f) Tobisu, M.; Hyodo, I.; Chatani, N. *J. Am. Chem. Soc.* **2009**, *131*, 12070. (g) Aihara, Y.; Chatani, N. *J. Am. Chem. Soc.* **2013**, *135*, 5308. (h) Song, W.; Lackner, S.; Ackermann, L. *Angew. Chem., Int. Ed.* **2014**, *53*, 2477.
- (8) Kleiman, J. P.; Dubeck, M. *J. Am. Chem. Soc.* **1963**, *85*, 1544.
- (9) Zargarian, D. *Coord. Chem. Rev.* **2002**, 233, 157.
- (10) (a) Ceder, R. M.; Granell, J.; Muller, G. *J. Chem. Soc., Dalton Trans.* **1998**, 1047. (b) Ceder, R. M.; Granell, J.; Muller, G.; Font-Bardia, M.; Solans, X. *Organometallics* **1995**, *14*, 5544. (c) Ceder, R. M.; Granell, J.; Muller, G.; Font-Bardía, M.; Solans, X. *Organometallics* **1996**, *15*, 4618.
- (11) Muller, G.; Panyella, D.; Rocamora, M.; Sales, J.; Font-Bardía, M.; Solans, X. *J. Chem. Soc., Dalton Trans.* **1993**, 2959.
- (12) Ruhland, K.; Obenhuber, A.; Hoffmann, S. D. *Organometallics* **2008**, *27*, 3482.
- (13) Cámpora et al. have also reported imidoyl complexes prepared by insertion of ArNC or CO into the Ni-bimetallic species $\text{trans}-(\text{Me}_3\text{P})\text{BrNi}(\mu_2-\eta^3-\eta^1-\text{CH}_2\text{-}o\text{-C}_6\text{H}_4)\text{NiBr}(\text{PMe}_3)_2$: (a) Cámpora, J.; Gutierrez, E.; Monge, A.; Poveda, M. L.; Ruiz, C.; Carmona, E. *Organometallics* **1993**, *12*, 4025. (b) Cámpora, J.; Gutierrez, E.; Monge, A.; Poveda, M. L.; Carmona, E. *Organometallics* **1992**, *11*, 2644.
- (14) (a) Pandarus, V.; Zargarian, D. *Chem. Commun.* **2007**, 978. (b) Pandarus, V.; Zargarian, D. *Organometallics* **2007**, *26*, 4321. (c) Salah, A. B.; Zargarian, D. *Dalton Trans.* **2011**, 40, 8977. (d) Salah, A. B.; Offenstein, C.; Zargarian, D. *Organometallics* **2011**, *30*, 5352. (e) Lefèvre, X.; Spasyuk, D. M.; Zargarian, D. *J. Organomet. Chem.* **2011**, *696*, 864. (f) Lefèvre, X.; Durieux, G.; Lesturgez, S.; Zargarian, D. *J. Mol. Catal. A* **2011**, *335*, 1. (g) Vabre, B.; Lindperg, F.; Zargarian, D. *Green Chem.* **2013**, *15*, 3188. (h) Hao, J.; Mougang-Soumé, B.; Vabre, B.; Zargarian, D. *Angew. Chem., Int. Ed.* **2014**, *53*, 3218–3222. (i) Hao, J.; Vabre, B.; Mougang-Soumé, B.; Zargarian, D. *Chem. Eur. J.* **2014**, *20*, 12544. (j) Vabre, B.; Petiot, P.; Declercque, R.; Zargarian, D. *Organometallics* **2014**, *33*, 5173.
- (15) Gulevich, A. V.; Melkonyan, F. S.; Sarkar, D.; Gevorgyan, V. *J. Am. Chem. Soc.* **2012**, *134*, 5528.
- (16) Reaction of ethylene with Ru–phosphinite complexes obtained from C–H ortho metalation provided one of the earliest examples of ortho alkylation of phenol via ethylene insertion: Lewis, L. N.; Smith, J. F. *J. Am. Chem. Soc.* **1986**, *108*, 2728.
- (17) Bedford, R. B.; Coles, S. J.; Hursthouse, M. B.; Limmert, M. E. *Angew. Chem., Int. Ed.* **2003**, *42*, 112.
- (18) Bedford, R. B.; Hazelwood (née Welch), S. L.; Horton, P. N.; Hursthouse, M. B. *Dalton Trans.* **2003**, 4164.
- (19) Vabre, B.; Spasyuk, D. M.; Zargarian, D. *Organometallics* **2012**, *31*, 8561–8570.
- (20) Zargarian, D.; Castonguay, A.; Spasyuk, D. M.; van Koten, G.; Milstein, D. ECE-Type Pincer Complexes of Nickel. *Top. Organomet. Chem.* **2013**, *40*, 131–174.
- (21) Jiménez-Tenorio, M.; Puerta, M. C.; Salcedo, I.; Valerga, P.; Costa, S. I.; Silva, L. C.; Gomes, P. T. *Organometallics* **2004**, *23*, 3139.

(22) (a) Li, J.; Lutz, M.; Spek, A. L.; van Klink, G. P. M.; van Koten, G.; Klein Gebbink, R. J. M. *J. Organomet. Chem.* **2010**, *695*, 2618. (b) Bedford, R. B.; Hazelwood (née Welch), S. L.; Limmert, M. E.; Albisson, D. A.; Draper, S. M.; Scully, P. N.; Coles, S. J.; Hursthouse, M. B. *Chem. Eur. J.* **2003**, *9*, 3216.

(23) (a) Dinger, M. B.; Scott, M. J. *Inorg. Chem.* **2001**, *40*, 856. (b) Cobley, C. J.; Ellis, D. D.; Orpen, A. G.; Pringle, P. G. *J. Chem. Soc., Dalton Trans.* **2000**, 1101. (c) Ng, J. K.-P.; Chen, S.; Tan, G.-K.; Leung, P.-H. *Eur. J. Inorg. Chem.* **2007**, *2007*, 3124–3134.

(24) Boutadla, Y.; Davies, D. L.; Macgregor, S. A.; Poblador-Bahamonde, A. I. *Dalton Trans.* **2009**, 5820.

(25) Care was taken to ensure that all samples were treated in the same manner. The AB doublets emerging over time in the $^{31}\text{P}\{^1\text{H}\}$ NMR spectra and attributed to the cyclometalated complexes **3b–d** were used to estimate the extent of cyclometalation. This was done on the basis of integration against the signal for the internal standard PPh_3 contained in a carefully prepared sealed capillary that was used for all samples.

(26) Vabre, B.; Lambert, M. L.; Petit, A.; Ess, D. H.; Zargarian, D. *Organometallics* **2012**, *31*, 6041.

(27) Kalyani, D.; Sanford, M. S. *Org. Lett.* **2005**, *7*, 4149.

(28) Edwards, A. J.; Macgregor, S. A.; Rae, A. D.; Wenger, E.; Willis, A. C. *Organometallics* **2001**, *20*, 2864.

(29) Nagashima, H.; Tanabiki, M. Patent Application, EP 1241175 A2, 2002.

(30) For a very recent example of Ni-based methodology for functionalizing C–H bonds with aliphatic electrophiles, see: Song, W.; Lackner, S.; Ackermann, L. *Angew. Chem., Int. Ed.* **2014**, *53*, 2477–2480.

(31) SAINT, *Integration Software for Single Crystal Data, Release 6.06*; Bruker AXS Inc., Madison, WI, 1999.

(32) Sheldrick, G. M. SADABS, *Bruker Area Detector Absorption Corrections*; Bruker AXS Inc., Madison, WI, 1999.

(33) XPREP, *X-ray Data Preparation and Reciprocal Space Exploration Program, Release 5.10*; Bruker AXS Inc., Madison, WI, 1997.

(34) SHELXTL; *The Complete Software Package for Single Crystal Structure Determination, Release 5.10*; Bruker AXS Inc., Madison, WI, 1997.

(35) (a) Sheldrick, G. M. SHELXS97, *Program for the Solution of Crystal Structures*; University of Gottingen, Gottingen, Germany, 1997. (b) Sheldrick, G. M. SHELXL97, *Program for the Refinement of Crystal Structures*; University of Gottingen, Gottingen, Germany, 1997.